JOURNAL OF BACTERIOLOGY, Apr. 2007, p. 2610–2617 Vol. 189, No. 7
0021-9193/07/$08.00+0 doi:10.1128/JB.01539-06

MalE of Group A *Streptococcus* Participates in the Rapid Transport of Maltotriose and Longer Maltodextrins▽†

Samuel A. Shelburne III,[1] Han Fang,[2] Nnaja Okorafor,[1] Paul Sumby,[3] Izabela Sitkiewicz,[3] David Keith,[1] Payal Patel,[3] Celest Austin,[4] Edward A. Graviss,[4] James M. Musser,[3]* and Dar-Chone Chow[2,5]*

Section of Infectious Diseases, Department of Medicine, Baylor College of Medicine, Houston, Texas, 77030[1]; Department of Chemistry, University of Houston, Houston, Texas, 77024[2]; Center for Molecular and Translational Human Infectious Diseases Research, The Methodist Hospital Research Institute, Houston, Texas, 77030[3]; and Department of Pathology[4] and Structural and Computational Biology and Molecular Biophysics Program,[5] Baylor College of Medicine, Houston, Texas 77030

Received 3 October 2006/Accepted 11 January 2007

Study of the maltose/maltodextrin binding protein MalE in *Escherichia coli* has resulted in fundamental insights into the molecular mechanisms of microbial transport. Whether gram-positive bacteria employ a similar pathway for maltodextrin transport is unclear. The maltodextrin binding protein MalE has previously been shown to be key to the ability of group A *Streptococcus* (GAS) to colonize the oropharynx, the major site of GAS infection in humans. Here we used a multifaceted approach to elucidate the function and binding characteristics of GAS MalE. We found that GAS MalE is a central part of a highly efficient maltodextrin transport system capable of transporting linear maltodextrins that are up to at least seven glucose molecules long. Of the carbohydrates tested, GAS MalE had the highest affinity for maltotriose, a major breakdown product of starch in the human oropharynx. The thermodynamics and fluorescence changes induced by GAS MalE-maltodextrin binding were essentially opposite those reported for *E. coli* MalE. Moreover, unlike *E. coli* MalE, GAS MalE exhibited no specific binding of maltose or cyclic maltodextrins. Our data show that GAS developed a transport system optimized for linear maltodextrins longer than two glucose molecules that has several key differences from its well-studied *E. coli* counterpart.

Analysis of microbial carbohydrate physiology has been a fertile area of scientific research for many decades. Fundamental discoveries in the areas of transcriptional regulation, selective nutrient utilization, and molecular transport have been derived from studies of microbial carbohydrate acquisition and processing (13, 27, 34). For example, the uptake and utilization of maltose/maltodextrins by *Escherichia coli* has become a model for understanding how microbes transport and use complex sugars (3).

The study of *E. coli* MalE, the periplasmic substrate binding protein of the maltose/maltodextrin ATP binding cassette transporter, has been a particularly fruitful area of investigation (32, 33). Although *E. coli* MalE binds to a variety of α-1,4-linked oligoglucosides, including linear, cyclic, reduced, and oxidized maltodextrins, only a portion of the bound ligands is subsequently transported into the cell (10). The interaction of purified *E. coli* MalE with the actively transported substrates maltose and maltotriose causes an increase in the *E. coli* MalE maximum emission wavelength (10, 39). The change in the fluorescence emission spectrum correlates with the closed and open forms of the *E. coli* MalE-ligand complex (8). The closed form is needed for active transport to occur (11). The binding of *E. coli* MalE to substrates that are actively transported results in an endothermic reaction that is entropy driven (40). Conversely, the binding of *E. coli* MalE to nontransported substrates is exothermic and results in a decrease in the maximum fluorescence emission wavelength of *E. coli* MalE (9, 40). Therefore, study of *E. coli* MalE has generated data showing two major modes of ligand binding: one in which an endothermic reaction driven by entropy results in active transport and one in which an exothermic reaction fails to result in transport of the bound ligand.

Investigation of maltose/maltodextrin utilization by gram-positive bacteria initially lagged behind investigation of maltose/maltodextrin utilization by *E. coli* but has accelerated recently as fundamental distinctions have been recognized (16, 21, 28). In contrast to the freely diffusible periplasmic location of *E. coli* MalE, gram-positive bacterial homologues of *E. coli* MalE are putative lipoproteins whose amino termini are anchored in the cell membrane (38). Isogenic mutant strains of various gram-positive bacteria in which genes encoding putative maltodextrin binding proteins were inactivated were still able to utilize and/or transport maltose but not maltotriose (23, 31). Moreover, a recent study found that the purified MalE homolog from *Bacillus subtilis* had far greater affinity for maltotriose than for maltose, suggesting that the binding spectrum is different than that of *E. coli* MalE (31).

Our laboratory focuses on understanding how the gram-

* Corresponding author. Mailing address for James M. Musser: Center for Molecular and Translational Human Infectious Diseases Research, The Methodist Hospital Research Institute, B490, 6565 Fannin Street, Houston, TX 77030. Phone: (713) 441-5890. Fax: (713) 441-3447. E-mail: jmmusser@tmh.tmc.edu. Mailing address for Dar-Chone Chow: Department of Chemistry, University of Houston, 136 Fleming Building, Houston, TX 77024. Phone: (713) 743-1798. Fax: (713) 743-2709. E-mail: dchow@mail.uh.edu.

† Supplemental material for this article may be found at http://jb.asm.org/.

▽ Published ahead of print on 26 January 2007.

positive bacterium group A *Streptococcus* (GAS) causes diverse infections in humans (20). Recently, we have performed genome-wide transcriptome analyses of GAS during various phases of host-pathogen interactions, such as growth in human blood and saliva and infection of mouse soft tissue and the nonhuman primate oropharynx (7, 8, 29, 41). The transcript levels of M5005_spy1058, the gene coding for a putative homolog of *E. coli* MalE, were consistently elevated in these investigations, suggesting that M5005_SPy1058 has a role in host-pathogen interactions. Antibodies to M5005_SPy1058 were found in humans recovering from GAS infections and in mice experimentally infected with GAS, demonstrating that M5005_SPy1058 is produced during infection and stimulates an immune response (17). A subsequent investigation showed that M5005_SPy1058 participates in the earliest stages of GAS colonization of the oropharynx (31).

Based on homology with *E. coli* MalE (26% amino acid identity and 42% similarity), M5005_SPy1058 has also been annotated MalE (2, 6). To better understand how GAS MalE contributes to GAS colonization of the oropharynx, we analyzed GAS MalE utilizing a multifaceted approach. We employed complementary modalities to investigate the binding characteristics and substrate specificity of purified GAS MalE. Using a Δ*malE* isogenic mutant strain, we correlated the observed binding properties with growth characteristics and performed nutrient uptake assays to elucidate the role played by MalE in global GAS physiology. Our investigations show that GAS MalE-ligand binding has properties distinct from those observed for *E. coli* MalE, perhaps because of a difference in nutrient availability at the site of host-pathogen interaction. The differences in the maltodextrin binding proteins of GAS and *E. coli* demonstrated here suggest that there were diverse evolutionary pressures in the development of bacterial carbohydrate binding strategies.

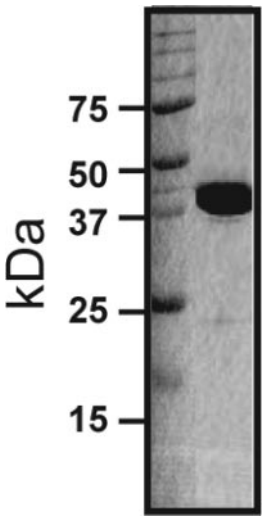

FIG. 1. Sodium dodecyl sulfate-polyacrylamide gel electrophoresis analysis of purified recombinant GAS MalE. GAS MalE was cloned and overexpressed in *E. coli* and then purified to apparent homogeneity as described in Materials and Methods. Proteins were separated on a 12% polyacrylamide gel.

MATERIALS AND METHODS

Bacterial strains. The genome of serotype M1 strain MGAS5005 has been completely sequenced (37). Strain MGAS5005 has been studied extensively with animal models of GAS infection and in vitro, and the studies have included transcriptome analysis during growth in human saliva (7, 30, 36, 41). The Δ*malE* isogenic mutant strain is an MGAS5005 derivative in which nearly the entire *malE* open reading frame is replaced by a spectinomycin (*spc*) resistance cassette in a nonpolar fashion (31). The comp*ΔmalE* strain is a genetically complemented derivative of the Δ*malE* strain in which the *malE* open reading frame plus the promoter region is present in *trans* (31).

Culture media. GAS was grown on Trypticase soy agar containing 5% sheep blood agar (Becton Dickinson) or in Todd-Hewitt broth containing 0.2% (wt/vol) yeast extract (THY) (Difco). Various carbohydrates were added at a concentration of 0.5% (wt/vol) to a carbohydrate-free preparation of a commercially available chemically defined medium (CDM) (JR Biosciences) (42). We have shown previously that GAS does not grow in the carbohydrate-free CDM when no exogenous carbohydrate is added (31). In this paper, we use the terms glucose-medium, maltose-medium, maltotriose-medium, etc. to refer to the carbohydrate-free CDM with a specific carbohydrate added at a concentration of 0.5%.

Growth of GAS strains in various media. All growth experiments were done at least in quadruplicate. For comparison growth studies using THY or CDM, GAS strains were grown overnight in THY. An overnight culture was added to fresh medium to obtain a uniform starting optical density at 600 nm (OD_{600}) of 0.01, generally about 1:100 dilution. The spectrophotometric density was then determined hourly until completion of the experiment. GAS was grown in human saliva as described previously (30). Saliva was collected on ice from healthy volunteers as described in a Baylor College of Medicine Institutional Review Board human subjects protocol (30). Pooled saliva collected from at least four donors was used to minimize the effects of donor variation on the study results.

Carbohydrate transport assays. Strains MGAS5005, Δ*malE*, and comp*ΔmalE* were grown to the mid-exponential phase in CDM with the carbohydrate of interest added at a concentration of 0.5%. The bacteria were collected by centrifugation, washed, and suspended to obtain an OD_{600} of 0.5 in 160 μl CDM lacking carbohydrates. Under these conditions a 1-ml suspension contained 1.75×10^8 GAS CFU. [^{14}C]glucose (300 mCi/mmol; 200 μCi/ml), [^{14}C]maltose (600 mCi/mmol; 200 μCi/ml), and [^{14}C]maltotriose (900 mCi/mmol; 100 μCi/ml) were purchased from American Radiolabeled Chemicals, St. Louis, MO. [^{14}C]maltose was determined to be >98% pure by thin-layer chromatography, whereas [^{14}C]maltotriose was found to be ~90% pure (American Radiolabeled Chemicals, personal communication). Forty microliters of a ^{14}C-labeled sugar was added to GAS cells at 37°C to obtain a final volume of 200 μl and a final concentration of radiolabeled carbohydrate of 20 μM. At different times 40-μl samples were removed and filtered on a 0.45-μm nitrocellulose membrane (Millipore), which was then rinsed twice with CDM lacking carbohydrates. Liquid scintillation counting was used to determine the radioactivity retained on each filter (Beckman model LS7500). For competition experiments, cells harvested in the mid-exponential growth phase were suspended in CDM containing 100 μM unlabeled carbohydrate prior to addition of the radiolabeled carbohydrate. For kinetic studies, the final ^{14}C-labeled sugar concentration was varied from 10 nM to 50 μM. Samples were taken every 30 s for the first 120 s, a period during which carbohydrate transport rates were found to be linear. All experiments were performed in quadruplicate on at least two separate occasions.

GAS MalE overexpression and purification. The GAS *malE* gene encoding a protein which lacked the putative secretion signal sequence and in which the N-terminal cysteine was replaced by a glycine residue was previously cloned into *E. coli* (17). Recombinant, soluble GAS MalE was overexpressed and purified to apparent homogeneity as described previously, using the following modifications (17). Briefly, the cell paste was resuspended in 10 mM Tris–1 mM EDTA (pH 8.0) and sonicated on ice for 15 min. The sample was centrifuged at 60,000 × *g* for 30 min to pellet the cell debris and insoluble material. The NaCl concentration in the clarified lysate was adjusted to 100 mM, and the lysate was passed through a DEAE column to absorb the unwanted material. The pass-through material was diluted 15-fold and passed through a HiTrap Q column (GE Healthscience). GAS MalE eluted between 45 and 150 mM NaCl on a 10 to 500 mM NaCl gradient. After this the eluted GAS MalE was purified further to apparent homogeneity using sizing chromatography (Fig. 1).

Fluorescence spectroscopy. Fluorescence spectra were recorded with a Perkin-Elmer model 204 fluorescence spectrophotometer that was connected to a computer for digital recording. The excitation wavelength was 275 nm, and the emission spectrum was scanned from 290 to 350 nm. An excitation wavelength of

TABLE 1. Growth of strain MGAS5005 in various media

Carbon source[a]	Doubling time (min)[b]	Final absorption (mean ± SD)[c]
THY	51.2	1.421 ± 0.073
Glucose	57.2	1.214 ± 0.121
Maltose	73.2	0.712 ± 0.052
Maltotriose	59.6	1.266 ± 0.082
Maltotetraose	64.3	1.144 ± 0.105
Maltoheptaose	63.9	1.112 ± 0.081
Maltohexaose	61.7	1.151 ± 0.114
Maltoheptaose	65.4	1.141 ± 0.092
Lactose	72.6	0.727 ± 0.081
Sucrose	69.4	0.925 ± 0.031

[a] Carbon sources were added at a concentration of 0.5% (wt/vol) to carbohydrate-free chemically defined medium.
[b] The doubling time was determined during the logarithmic phase of growth.
[c] The final absorption value is the OD_{600} in the stationary phase of growth.

275 nm was the maximum excitation wavelength based on the excitation scan (see Fig. S1 in the supplemental material). The maximum emission wavelength was determined from the scanned spectrum using curve fitting.

Isothermal titration calorimetry. Isothermal titration calorimetry (ITC) measurements were obtained with a VP-ITC calorimeter (MicroCal LLC). The purified protein was exchanged with the appropriate buffer (10 mM Tris [pH 8.0]–150 mM NaCl or 10 mM phosphate [pH 8.0]–150 mM NaCl) using sizing chromatography. The same buffer was used to dissolve the solid carbohydrates to obtain the desired concentrations. Typically, the protein was loaded into the sample cell (volume, 1.4 ml) at a concentration of 5 to 10 μM. The maltodextrin solutions were loaded into the injection syringe at a concentration between 50 and 100 μM. The typical amount injected was 8 to 10 μl, and the total injection volume was 290 μl with 300-s spacing between consecutive injections. The injection syringe was stirred at 290 rpm. The data were analyzed using Origin 7.0 (OriginLab) with an ITC customer add-on. The software analysis included consideration of the stepwise dilution.

Statistical analysis. Growth data were compared using analysis of variance. The results of radiolabeled carbohydrate uptake assays performed with 20 μM carbohydrate were compared using linear regression. Apparent K_m and V_{max} values for glucose, maltose, and maltotriose were calculated by nonlinear regression using GraphPad Prism 4 and the following equation: $Y = (V_{max} \times X)/(K_m + X)$. Statistical significance was assigned at a P value of 0.05 using Bonferroni's adjustments for multiple comparisons when appropriate. Statistical calculations were performed with the NCSS software, version 2004.

RESULTS

Strain MGAS5005 exhibits robust growth in maltodextrins longer than maltose. In a previous investigation we found that the GAS serotype M1 strain MGAS5005 grew in a chemically defined medium with maltose as the sole carbon source (referred to as maltose-medium here) at a rate that was lower than the rate in glucose-medium and to a lower final density (31). Surprisingly, we found that strain MGAS5005 grew faster and to a higher final density in maltotriose-medium than in maltose-medium (Table 1). The growth of strain MGAS5005 in maltotriose-medium was essentially identical to the growth in a medium containing glucose, the preferred carbon source for many bacteria (Table 1) (24, 35). Importantly, the major habitat for GAS in humans, the oropharynx, has high levels of maltotriose and maltodextrins longer than glucose and maltose as a result of starch breakdown by salivary α-amylase (14, 19). We next determined whether the rapid growth of strain MGAS5005 in maltotriose-medium was also observed in media with longer maltodextrins as the sole carbon sources. The doubling times and final concentrations of strain MGAS5005 in maltotetraose-, maltopentaose-, maltohexaose-, and maltoheptaose-media were not statistically different than those in maltotriose- or glucose-medium (Table 1). In contrast, compared to growth with maltotriose or glucose, we observed increased doubling times and lower final concentrations when strain MGAS5005 was grown in lactose- or sucrose-medium. These data indicate that strain MGAS5005 is able to utilize maltodextrins longer than maltose in a highly efficient manner, resulting in growth that is faster and more robust than growth with either maltose or other disaccharides.

TABLE 2. Transport of ^{14}C-labeled sugars by group A *Streptococcus*

Strain	Apparent K_m (μM)/V_{max} (nmol/min/10^{10} CFU)[a]		
	Glucose	Maltose	Maltotriose
MGAS5005	4.5/135	12.5/67	2.1/127
Δ*malE*	4.3/131	16.3/43	17.3/41
comp*malE*	5.1/142	11.5/72	1.9/139

[a] Apparent K_m values were determined by assuming that transport follows Michaelis-Menton kinetics.

V_{max} of strain MGAS5005 for labeled maltotriose is higher than V_{max} for maltose. We previously established that strain MGAS5005 transports less maltose than glucose when the concentration of labeled carbohydrate is 20 μM (31). To obtain further insight into the transport kinetics of glucose, maltose, and maltotriose in strain MGAS5005, we determined K_m and V_{max} values for the three carbohydrates using concentrations ranging from 10 nM to 50 μM. Of the three sugars tested, maltotriose had the lowest apparent K_m (2.1 μM) (Table 2). The maximum uptake rates for maltotriose and glucose were not statistically different, whereas the V_{max} for maltose was significantly different than the V_{max} for either glucose or maltotriose ($P < 0.001$). Therefore, we concluded that the uptake of radiolabeled maltotriose by strain MGAS5005 is faster than the uptake of maltose and similar to the uptake of glucose.

MalE is needed for optimum growth of strain MGAS5005 in maltodextrin-media. In a previous study, nonpolar inactivation of GAS *malE* decreased growth in maltose-medium without affecting growth in nutrient-rich broth or in glucose-medium (31). In maltotriose-medium, strain MGAS5005 and the comp*malE* strain grew to final densities that were more than twice that of the Δ*malE* isogenic mutant strain (Fig. 2A; see Table S1 in the supplemental material). Importantly, the Δ*malE* isogenic mutant strain was essentially unable to grow in media in which the maltodextrin supplied was longer than maltotriose (Fig. 2B; see Table S1 in the supplemental material), whereas the wild-type and complemented strains grew equally well. We observed no differences in growth of the three stains in a medium containing either lactose or sucrose (see Table S1 in the supplemental material). These data indicate that MalE is needed for the optimal growth of strain MGAS5005 in various media containing maltodextrins but is not involved in the utilization of lactose or sucrose.

MalE is needed for optimum transport of maltotriose. To test whether MalE participates in the transport of maltotriose, we determined the K_m and V_{max} values for maltotriose for the wild-type, Δ*malE*, and comp*malE* strains. The V_{max} of the Δ*malE* strain for maltotriose was approximately one-third the V_{max} of the MGAS5005 or comp*malE* strain for maltotriose (Table 2). Similarly, inactivation of *malE* led to an increase in

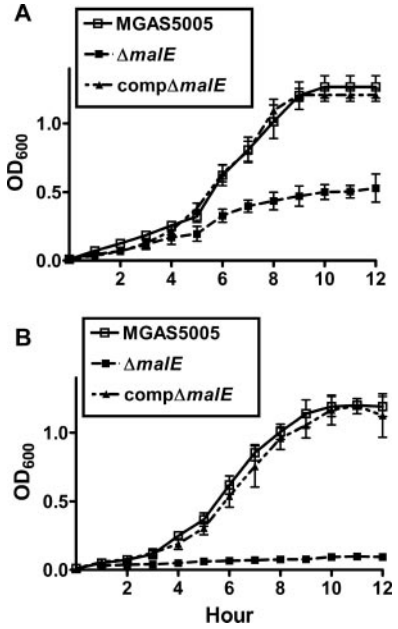

FIG. 2. MalE is vital to the ability of GAS to utilize maltodextrins. OD_{600} values were determined at different times during growth in a carbohydrate-free chemically defined medium supplemented with either 0.5% (wt/vol) maltotriose (A) or 0.5% (wt/vol) maltotetraose (B). The data are means ± standard deviations for five independent experiments.

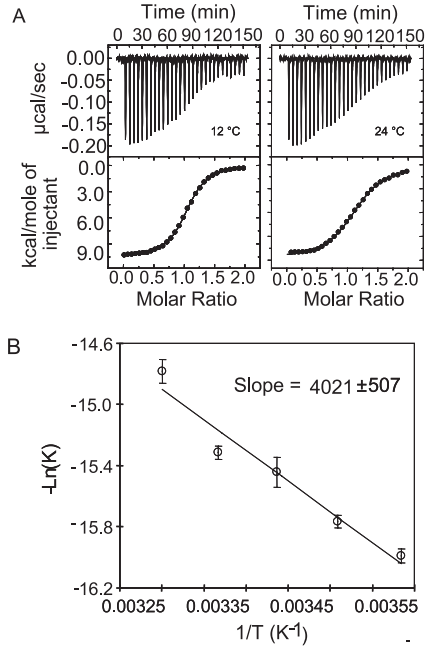

FIG. 3. GAS MalE binds maltotriose with submicromolar affinity in an enthalpy-driven reaction. (A) Negative binding enthalpy demonstrated by representative ITC curves for GAS MalE binding with maltotriose at 12 and 24°C. (B) Plot of $-\ln(K)$ versus $1/T$, showing a linear relationship. The van't Hoff enthalpy was calculated from the slope of the linear relationship to be $-8.0 \times 10^3 \pm 1.0 \times 10^3$ cal/mol.

the apparent K_m for maltotriose, from 2.1 μM in strain MGAS5005 to 17.3 μM. Finally, consistent with previous observations, the Δ*malE* strain had slightly increased K_m and decreased V_{max} values for maltose compared with the strain MGAS5005 values (Table 2) (31). These data indicate that MalE is required for the majority of but not all maltotriose uptake by strain MGAS5005 and that MalE affects the uptake of maltose, a finding consistent with our previous growth data (31).

Inability to detect specific GAS MalE binding to maltose. *E. coli* MalE binds maltose with a half-maximum concentration (K_d) of ~1 μM in an enthalpy-unfavorable, entropy-driven reaction that results in an increase in the *E. coli* MalE maximum emission wavelength (9, 10, 40). Surprisingly, when maltose was added to purified GAS MalE, we were unable to detect a change in the shape of the GAS MalE fluorescence emission spectrum, although the emission intensity appeared to be slightly lower (data not shown). However, we were unable to reliably estimate the decrease in the GAS MalE fluorescence intensity with maltose because of a high degree of variability in repeated measurements. Moreover, the decrease in the GAS MalE fluorescence intensity with maltose was not saturable. Even after addition of millimolar amounts of maltose, we continued to observe a decrease in the fluorescence emission intensity. Next we performed ITC titration of maltose into GAS MalE at several different temperatures to be sure that we were not performing fluorescence spectroscopy at the isoenthalpic temperature. This titration produced no discernible evidence of binding between GAS MalE and maltose (data not shown). We concluded that the interaction between maltose and GAS MalE is nonspecific and either heat silent or too weak to be detected by our methodology.

Purified GAS MalE binds maltotriose with submicromolar affinity in an enthalpy-driven reaction. To obtain further insight into the molecular basis of GAS maltodextrin transport, we carried out biophysical characterization of the interactions between the purified GAS MalE protein and various linear maltodextrins longer than two glucose molecules. We initially employed ITC measurements to determine the binding free energy, binding enthalpy, binding entropy, and stoichiometry of GAS MalE and various linear maltodextrins. Figure 3A shows representative raw ITC data for maltotriose titrated into GAS MalE at 12 and 24°C. The data suggest a 1:1 binding model for GAS MalE-maltotriose at submicromolar affinity (0.14 to 0.42 μM) (see Table S2 in the supplemental material). In the temperature range used for our measurements (6 to 30°C), the binding of maltotriose by GAS MalE was enthalpy (ΔH) driven and entropy (ΔS) unfavorable. The enthalpy was almost independent of temperature (T), with a value of $-10.7 \times 10^3 \pm 0.3 \times 10^3$ cal/mol. The estimated binding heat capacity of GAS MalE-maltotriose binding was minimal, with a value of -10 ± 20 cal/mol/K (degrees Kelvin). These data are essentially opposite those observed for *E. coli* MalE-maltotriose binding, which is enthalpy unfavorable and entropy driven (40).

We also analyzed the temperature dependence of the affinity of GAS MalE for maltotriose at temperatures ranging from 6 to 30°C (Fig. 3B). We calculated the van't Hoff enthalpy (directly related to the slope of ln K [binding affinity] versus $1/T$) by determining the relationship between temperature and the

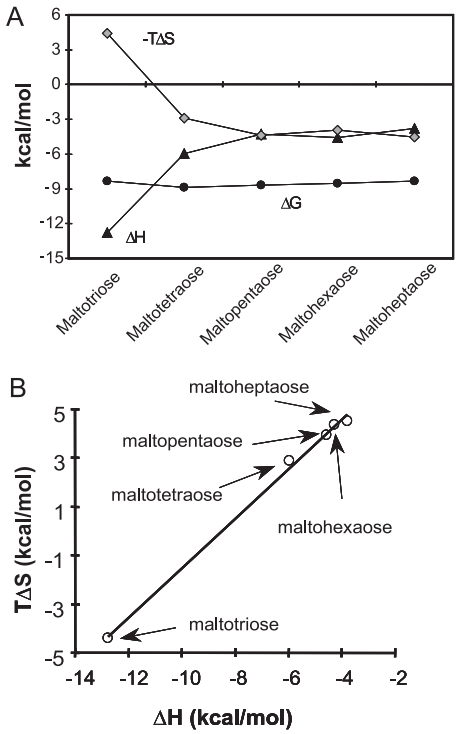

FIG. 4. Enthalpy-entropy compensation. (A) Plots of ΔG (●), ΔH (▲), and $-T\Delta S$ (◆) versus maltodextrins. The data show two trends of enthalpy changes depending on the number of glucose units; one is the rapid change from maltotriose to maltotetraose, showing the effect of extra glucose moiety binding, and the other is the lack of change from maltopentaose to maltoheptaose, indicating that the extra glucose no longer contacts the protein. (B) Plot of ΔH versus $T\Delta S$ for all the maltodextrins with a slope of 1, suggesting that there is an enthalpy-entropy compensation effect that results in minimal change in the total binding free energy.

binding affinity of GAS MalE for maltotriose. Analysis of the data generated yielded an estimated van't Hoff enthalpy of about $-8.0 \times 10^3 \pm 1.0 \times 10^3$ cal/mol (Fig. 3B). Considering the potential experimental errors, we believe that the results of the van't Hoff enthalpy calculation are close to the calorimetric enthalpy (less than 25% deviation from our ITC measurement, -11×10^3 cal/mol) (12), thereby confirming the thermodynamic measurements obtained initially.

GAS MalE binds linear maltodextrins up to seven glucose molecules long with submicromolar affinity. To characterize the interactions of GAS MalE with linear maltodextrins longer than maltotriose, we obtained ITC measurements for GAS MalE binding of maltotetraose, maltopentaose, maltohexaose, and maltoheptaose. GAS MalE had a binding affinity for each of the linear maltodextrins in the submicromolar range (Fig. 4). The binding of linear maltodextrins and GAS MalE is enthalpy favorable ($\Delta H < 0$) (see Table S3 in the supplemental material). As the length of the maltodextrin increased, the enthalpy driving force decreased and the entropy driving force (ΔS) increased in a compensatory fashion (Fig. 4). This resulted in about the same binding free energy (ΔG), suggesting that enthalpy-entropy compensation plays an important role. The finding that there is increasing entropy with increasing maltodextrin length is again directly opposite the results for *E. coli* MalE, for which enthalpy increases and entropy decreases when maltodextrins longer than maltose are bound (40).

GAS MalE binding of maltotriose and longer maltodextrins results in a decrease in the maximum intrinsic fluorescence wavelength. The maximum emission wavelength of *E. coli* MalE increases upon binding to linear maltodextrins (9–11). In light of our findings regarding the thermodynamics of GAS MalE-maltodextrin binding, we hypothesized that GAS MalE would exhibit a decrease in the maximum emission wavelength when it was bound to linear maltodextrins. GAS MalE alone had a typical bell-shaped emission spectrum with the maximum wavelength (λ_{max}) around 325 nm when it was excited with 275-nm light (Fig. 5A). When maltotriose was added to GAS MalE, the emission spectrum shifted such that the maximum fluorescence occurred around 315 nm (λ_{max}, 315 nm), a decrease compared to the wavelength observed with GAS MalE alone. When we plotted the change in λ_{max} versus the maltotriose concentration (Fig. 5B), the K_d of maltotriose was approximately 0.2 μM, which is very similar to the affinity determined using ITC. Two other longer maltodextrins, maltotetraose and maltopentaose, were tested using the same experimental setup (Fig. 5C and D). For maltotetraose and maltopentaose, the binding affinities calculated using fluorescence spectroscopy were again quite similar to those obtained using ITC (0.3 and 0.4 μM). Therefore, similar to *E. coli* MalE, the binding of linear maltodextrins to GAS MalE results in a shift in the maximum fluorescence intensity, indicating that a conformational change occurs upon maltodextrin binding (10). However, the fluorescence shift induced in GAS MalE is opposite that observed with *E. coli* MalE, a finding consistent with the dissimilarities observed in the binding thermodynamics of the two proteins.

GAS MalE does not strongly interact with β-cyclomaltodextrin, and GAS is unable to utilize cyclomaltodextrins for growth. A hallmark of *E. coli* MalE is its ability to bind to a variety of α-1,4-linked oligoglucosides, such as cyclic maltodextrins (9, 40). Serotype M1 strain MGAS5005 produces proteins putatively involved in the creation and utilization of cyclic maltodextrins (37). Therefore, we hypothesized that GAS MalE would be able to bind cyclic maltodextrins and that cyclic maltodextrins could serve as a nutrient source for GAS. However, similar to our findings with maltose, we were unable to detect binding of β-cyclomaltodextrin by GAS MalE using either ITC or fluorescence spectroscopy (data not shown). Analogous to our results with maltose, addition of β-cyclomaltodextrin to GAS MalE resulted in a decrease in the maximum fluorescence intensity that was not saturable, indicating that there was a nonspecific reaction. Moreover, when α-, β-, or γ-cyclomaltodextrin was the sole carbon source in a chemically defined medium, we detected no discernible growth of strain MGAS5005 (see Table S1 in the supplemental material). Therefore, we concluded that unlike *E. coli* MalE, GAS MalE does not interact appreciably with β-cyclomaltodextrins.

Transport of maltotriose is not inhibited by the presence of maltose or β-cylcomaltodextrins. Our previous data indicated that the transport of maltotriose is primarily mediated by MalE and that the binding of MalE to maltotriose was very-high-affinity binding compared to maltose and β-cylcomaltodextrin binding. As expected, preincubation of GAS cells with unlabeled maltotriose led to nearly complete inhibition of labeled

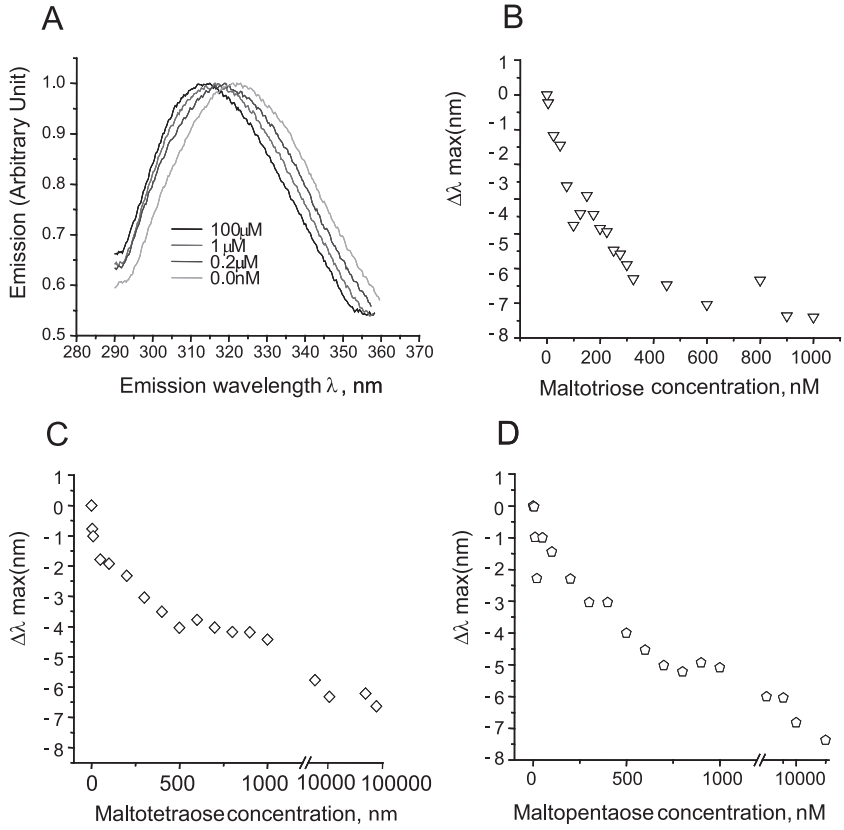

FIG. 5. Fluorescence spectroscopy analysis of GAS MalE-maltodextrin binding. The samples (0.5 μM GAS MalE protein) were excited with 275-nm UV light, and the emission spectra were scanned from 290 to 350 nm. The samples were added along with progressively higher concentrations of the maltodextrins, and then emission spectra were recorded. (A) Representative normalized GAS MalE fluorescence emission spectra with various maltotriose concentrations. (B to D) Plots of $\Delta\lambda_{max}$ versus concentrations of maltotriose (B), maltotetraose (C), and maltopentaose (D).

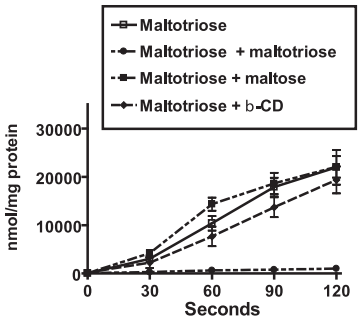

FIG. 6. Maltotriose uptake by GAS is not inhibited by maltose or β-cyclomaltodextrin. Serotype M1 strain MGAS5005 was grown to the mid-exponential phase in a carbohydrate-free CDM supplemented with 0.5% maltotriose. Cells were harvested by centrifugation, washed with carbohydrate-free CDM, and suspended to an OD_{600} of 0.5. Unlabeled ^{12}C-carbohydrates were added at a concentration of 100 μM prior to addition of [^{14}C]maltotriose at a final concentration of 20 μM. □, labeled maltotriose alone; ●, labeled maltotriose plus unlabeled maltotriose; ■, labeled maltotriose plus unlabeled maltose; ▲, labeled maltotriose plus unlabeled β-cylcomaltodextrin (β-CD). Samples were removed at the baseline and every 30 s for 120 s and passed through a 0.45-μm filter. The filters were washed twice with carbohydrate-free CDM, and liquid scintillation counting was used to determine the amount of radioactivity retained on each filter. The data are means ± standard deviations for four independent experiments.

maltotriose transport (Fig. 6; see Table S4 in the supplemental material). However, preincubation of GAS cells with either maltose or β-cyclodextrin did not significantly affect maltotriose uptake. On the basis of these findings together with our previous data, we concluded that, unlike *E. coli* MalE, GAS MalE has a much higher affinity for maltotriose than for maltose and β-cyclomaltodextrin that results in the preferential transport and utilization of linear maltodextrins longer than two glucose molecules.

DISCUSSION

GAS is the leading cause of human bacterial pharyngitis and may colonize the throat of up to 50% of school age children in nonepidemic periods (1, 22). Despite extensive study over many decades, much remains to be learned about the molecular mechanisms used by GAS to colonize and infect the human pharynx. The studies reported here were conducted to better understand the function of GAS MalE, a protein recently shown to be critical to GAS colonization of the oropharynx (31).

We were especially interested in comparing GAS MalE to its well-studied homolog in *E. coli*. There were several reasons to suspect that GAS MalE might have different structural and functional characteristics than *E. coli* MalE. First, the level of

homology at the amino acid level is relatively low (26% identity and 42% similarity). Second, most *E. coli* MalE is found free in the periplasmic space, whereas we have previously demonstrated that GAS MalE is found on the GAS cell surface, which is consistent with its predicted lipoprotein structure (17, 31). Finally, the overall structure of the GAS maltose gene region is distinct from that in *E. coli* (2, 6). No previous investigations of purified MalE or related homologues have been conducted with gram-positive human pathogens, and thus the ligand binding characteristics of GAS MalE were unknown prior to this investigation.

As predicted, we found some similarities and several notable differences between GAS MalE and *E. coli* MalE. First, like *E. coli* MalE, GAS MalE has the capacity to bind to maltotriose and maltodextrins up to and including maltoheptaose with high affinity (9). However, whereas *E. coli* MalE also binds maltose at a K_d of ~1 μM, we were unable to demonstrate GAS MalE maltose-specific binding even at millimolar concentrations of maltose (33). Moreover, in contrast to *E. coli*, we found that strain MGAS5005 grew more rapidly and to a higher final density when maltodextrins longer than two glucoses were the sole carbon source than when maltose was the sole carbon source (43).

We also found that GAS incorporated radiolabeled maltotriose more rapidly than it incorporated maltose and that the majority of maltotriose transport was MalE dependent. Therefore, we concluded that GAS MalE evolved to be highly efficient for transport of maltodextrins at least three glucose molecules long at the expense of maltose binding.

The most dramatic difference that we observed between GAS MalE and *E. coli* MalE was the nearly complete reversal of the thermodynamic and fluorescent properties of ligand binding. The interaction of *E. coli* MalE with ligands that are subsequently transported, such as maltose, maltotriose, or maltotetraose, results in an endothermic reaction and an increase in the maximum emission wavelength (9, 40). In contrast, GAS MalE binding to maltotriose and other transported ligands involved an exothermic reaction that resulted in a decrease in the maximum emission wavelength. These data suggest that the mechanism of maltodextrin binding by GAS MalE may be different from the mechanism employed by *E. coli* MalE. Interestingly, the findings for GAS MalE are quite similar to the findings obtained for hyperthermophilic prokaryotes, such as *Pyrococcus furiosus* (5, 26).

Our data raise the question of why GAS would evolve to produce a maltodextrin binding protein that optimally binds and initiates transport of maltotriose and longer maltodextrins at the expense of maltose and cyclic maltodextrins. One possible explanation was provided by a functional analysis of salivary α-amylase, the major starch-degrading protein present in the human oropharynx (25). Unlike pancreatic α-amylases, salivary α-amylase does not create a significant amount of glucose when it digests starch (14). Instead, the major products are maltose, maltotriose, maltotetraose, and longer maltodextrins. Importantly, maltotriose and longer maltodextrins make up more than 80% of the breakdown products resulting from starch digestion by salivary α-amylase, meaning that maltose production is limited (15, 19). Moreover, salivary α-amylase is unable to break down maltotriose, which allows large quantities to accumulate on dentition and in saliva following food ingestion (14, 15). Therefore, maltotriose and longer maltodextrins are relatively plentiful in the oropharynx compared to maltose and glucose, which may provide an explanation for why GAS developed a system tailored to the transport of longer maltodextrins. Another explanation for the relatively low affinity of GAS MalE for maltose is that GAS may employ an additional non-MalE pathway for maltose uptake. In recent studies of two gram-positive organisms, *Enterococcus faecalis* and *Bacillus subtilis*, workers found that maltose uptake was at least partially mediated by a phosphotransferase system (16, 28). Our data also suggest that there is a non-MalE pathway for maltose transport in GAS, meaning that there would be limited pressure on MalE to maintain a structure ideal for maltose uptake.

The data presented here raise several questions regarding maltose/maltodextrin in GAS. First, if purified GAS MalE does not bind maltose, why would the Δ*malE* strain exhibit decreased growth in a medium containing maltose and decreased uptake of radiolabeled maltose? GAS is known to have numerous known and putative carbohydrate metabolism enzymes on its cell surface (4). Therefore, one explanation for the effect of MalE on growth in a medium containing maltose is that GAS may convert maltose to maltodextrins that are subsequently transported via MalE. Another question raised by our data is, why does GAS not grow well in maltose-medium? It has been known for a long time that maltose augments intracellular iodophilic polysaccharide storage by GAS (18). It may be that maltose-induced iodophilic polysaccharide is detrimental to the growth of GAS. Finally, the fact that the Δ*malE* strain exhibits some transport of labeled maltotriose and growth on a medium containing maltotriose suggests that there may be another mechanism for transport of maltotriose into GAS other than a MalE-mediated pathway. Studies to further delineate maltose/maltodextrin transport and utilization by GAS are currently under way.

In conclusion, we studied the transport of malto- and cyclomaltodextrins by GAS MalE using a multimodal approach. Our study demonstrated that GAS MalE has a different binding spectrum and different binding characteristics than *E. coli* MalE. GAS evolved to produce a MalE protein that is highly efficient at transporting maltotriose and longer maltodextrins, perhaps because these carbohydrates are key nutrient sources for GAS in vivo. Further investigations of the mechanisms of microbial nutrient utilization are likely to yield new insights into host-pathogen interactions.

ACKNOWLEDGMENTS

We thank F. Quiocho and M. Pettitt for critical reading of the manuscript and M. Austermuehle and A. Davidson for their assistance in initiating the project.

This work was supported by American Heart Association grant 0565133Y to S.A.S., by Scientist Development Grant 0435186N to D.C., and by National Institutes of Health grant K12 RR 17655-04 to S.A.S. This work was also supported in part through startup funds from the University of Houston and the Institute for Molecular Design to D.C.

REFERENCES

1. **Bisno, A. L., G. S. Peter, and E. L. Kaplan.** 2002. Diagnosis of strep throat in adults: are clinical criteria really good enough? Clin. Infect. Dis. **35:**126–129.
2. **Blattner, F. R., G. Plunkett 3rd, C. A. Bloch, N. T. Perna, V. Burland, M.**

Riley, J. Collado-Vides, J. D. Glasner, C. K. Rode, G. F. Mayhew, J. Gregor, N. W. Davis, H. A. Kirkpatrick, M. A. Goeden, D. J. Rose, B. Mau, and Y. Shao. 1997. The complete genome sequence of *Escherichia coli* K-12. Science **277:**1453–1474.

3. **Boos, W., and H. Shuman.** 1998. Maltose/maltodextrin system of *Escherichia coli*: transport, metabolism, and regulation. Microbiol. Mol. Biol. Rev. **62:** 204–229.
4. **Cole, J. N., R. D. Ramirez, B. J. Currie, S. J. Cordwell, S. P. Djordjevic, and M. J. Walker.** 2005. Surface analyses and immune reactivities of major cell wall-associated proteins of group A streptococcus. Infect. Immun. **73:**3137–3146.
5. **Evdokimov, A. G., D. E. Anderson, K. M. Routzahn, and D. S. Waugh.** 2001. Structural basis for oligosaccharide recognition by *Pyrococcus furiosus* maltodextrin-binding protein. J. Mol. Biol. **305:**891–904.
6. **Ferretti, J. J., W. M. McShan, D. Ajdic, D. J. Savic, G. Savic, K. Lyon, C. Primeaux, S. Sezate, A. N. Suvorov, S. Kenton, H. S. Lai, S. P. Lin, Y. Qian, H. G. Jia, F. Z. Najar, Q. Ren, H. Zhu, L. Song, J. White, X. Yuan, S. W. Clifton, B. A. Roe, and R. McLaughlin.** 2001. Complete genome sequence of an M1 strain of *Streptococcus pyogenes*. Proc. Natl. Acad. Sci. USA **98:**4658–4663.
7. **Graham, M. R., K. Virtaneva, S. F. Porcella, W. T. Barry, B. B. Gowen, C. R. Johnson, F. A. Wright, and J. M. Musser.** 2005. Group A *Streptococcus* transcriptome dynamics during growth in human blood reveals bacterial adaptive and survival strategies. Am. J. Pathol. **166:**455–465.
8. **Graham, M. R., K. Virtaneva, S. F. Porcella, D. J. Gardner, R. D. Long, D. M. Welty, W. T. Barry, C. A. Johnson, L. D. Parkins, F. A. Wright, and J. M. Musser.** 2006. Analysis of the transcriptome of group A *Streptococcus* in mouse soft tissue infection. Am. J. Pathol. **169:**927–942.
9. **Hall, J. A., A. K. Ganesan, J. Chen, and H. Nikaido.** 1997. Two modes of ligand binding in maltose-binding protein of *Escherichia coli.* Functional significance in active transport. J. Biol. Chem. **272:**17615–17622.
10. **Hall, J. A., K. Gehring, and H. Nikaido.** 1997. Two modes of ligand binding in maltose-binding protein of *Escherichia coli.* Correlation with the structure of ligands and the structure of binding protein. J. Biol. Chem. **272:**17605–17609.
11. **Hall, J. A., T. E. Thorgeirsson, J. Liu, Y. K. Shin, and H. Nikaido.** 1997. Two modes of ligand binding in maltose-binding protein of *Escherichia coli.* Electron paramagnetic resonance study of ligand-induced global conformational changes by site-directed spin labeling. J. Biol. Chem. **272:**17610–17614.
12. **Horn, J. R., D. Russell, E. A. Lewis, and K. P. Murphy.** 2001. Van't Hoff and calorimetric enthalpies from isothermal titration calorimetry: are there significant discrepancies? Biochemistry (Moscow) **40:**1774–1778.
13. **Jacob, F., and J. Monod.** 1961. Genetic regulatory mechanisms in the synthesis of proteins. J. Mol. Biol. **3:**318–356.
14. **Kaczmarek, M. J., and H. Rosenmund.** 1977. The action of human pancreatic and salivary isoamylases on starch and glycogen. Clin. Chim. Acta **79:** 69–73.
15. **Kashket, S., J. Zhang, and J. Van Houte.** 1996. Accumulation of fermentable sugars and metabolic acids in food particles that become entrapped on the dentition. J. Dent. Res. **75:**1885–1891.
16. **Le Breton, Y., V. Pichereau, N. Sauvageot, Y. Auffray, and A. Rince.** 2005. Maltose utilization in *Enterococcus faecalis*. J. Appl. Microbiol. **98:**806–813.
17. **Lei, B., M. Liu, G. L. Chesney, and J. M. Musser.** 2004. Identification of new candidate vaccine antigens made by *Streptococcus pyogenes*: purification and characterization of 16 putative extracellular lipoproteins. J. Infect. Dis. **189:** 79–89.
18. **McFarland, C. R., T. L. Snyder, and R. McKenzie.** 1984. Polysaccharide storage in different streptococci. Microbios **40:**7–14.
19. **Mormann, J. E., and H. R. Muhlemann.** 1981. Oral starch degradation and its influence on acid production in human dental plaque. Caries Res. **15:** 166–175.
20. **Musser, J. M., and F. R. DeLeo.** 2005. Toward a genome-wide systems biology analysis of host-pathogen interactions in group A *Streptococcus*. Am. J. Pathol. **167:**1461–1472.
21. **Nieto, C., A. Puyet, and M. Espinosa.** 2001. MalR-mediated regulation of the *Streptococcus pneumoniae malMP* operon at promoter PM. Influence of a proximal divergent promoter region and competition between MalR and RNA polymerase proteins. J. Biol. Chem. **276:**14946–14954.
22. **Peter, G., and A. L. Smith.** 1977. Group A streptococcal infections of the skin and pharynx (second of two parts). N. Engl. J. Med. **297:**365–370.
23. **Puyet, A., A. M. Ibanez, and M. Espinosa.** 1993. Characterization of the *Streptococcus pneumoniae* maltosaccharide regulator MalR, a member of the LacI-GalR family of repressors displaying distinctive genetic features. J. Biol. Chem. **268:**25402–25408.
24. **Saier, M. H., Jr., S. Chauvaux, G. M. Cook, J. Deutscher, I. T. Paulsen, J. Reizer, and J. J. Ye.** 1996. Catabolite repression and inducer control in Gram-positive bacteria. Microbiology **142:**217–230.
25. **Scannapieco, F. A., G. Torres, and M. J. Levine.** 1993. Salivary alpha-amylase: role in dental plaque and caries formation. Crit. Rev. Oral Biol. Med. **4:**301–307.
26. **Schafer, K., U. Magnusson, F. Scheffel, A. Schiefner, M. O. Sandgren, K. Diederichs, W. Welte, A. Hulsmann, E. Schneider, and S. L. Mowbray.** 2004. X-ray structures of the maltose-maltodextrin-binding protein of the thermoacidophilic bacterium *Alicyclobacillus acidocaldarius* provide insight into acid stability of proteins. J. Mol. Biol. **335:**261–274.
27. **Schirmer, T., T. A. Keller, Y. F. Wang, and J. P. Rosenbusch.** 1995. Structural basis for sugar translocation through maltoporin channels at 3.1 A resolution. Science **267:**512–514.
28. **Schonert, S., S. Seitz, H. Krafft, E. A. Feuerbaum, I. Andernach, G. Witz, and M. K. Dahl.** 2006. Maltose and maltodextrin utilization by *Bacillus subtilis*. J. Bacteriol. **188:**3911–3922.
29. **Shelburne, S. A., P. Sumby, I. Sitkiewicz, C. N. Granville, F. R. DeLeo, and J. M. Musser.** 2005. Central role of a two-component gene regulatory system of previously unknown function in pathogen persistence in human saliva. Proc. Natl. Acad. Sci. USA **102:**16037–16042.
30. **Shelburne, S. A., III, C. Granville, M. Tokuyama, I. Sitkiewicz, P. Patel, and J. M. Musser.** 2005. Growth characteristics of and virulence factor production by group A *Streptococcus* during cultivation in human saliva. Infect. Immun. **73:**4723–4731.
31. **Shelburne, S. A., III, P. Sumby, I. Sitkiewicz, N. Okorafor, C. Granville, P. Patel, J. Voyich, R. Hull, F. R. Deleo, and J. M. Musser.** 2006. Maltodextrin utilization plays a key role in the ability of group A *Streptococcus* to colonize the oropharynx. Infect. Immun. **74:**4605–4614.
32. **Shilton, B. H., H. A. Shuman, and S. L. Mowbray.** 1996. Crystal structures and solution conformations of a dominant-negative mutant of *Escherichia coli* maltose-binding protein. J. Mol. Biol. **264:**364–376.
33. **Spurlino, J. C., G. Y. Lu, and F. A. Quiocho.** 1991. The 2.3-A resolution structure of the maltose- or maltodextrin-binding protein, a primary receptor of bacterial active transport and chemotaxis. J. Biol. Chem. **266:**5202–5219.
34. **Stulke, J., and W. Hillen.** 1999. Carbon catabolite repression in bacteria. Curr. Opin. Microbiol. **2:**195–201.
35. **Stulke, J., and W. Hillen.** 2000. Regulation of carbon catabolism in Bacillus species. Annu. Rev. Microbiol. **54:**849–880.
36. **Sumby, P., K. D. Barbian, D. J. Gardner, A. R. Whitney, D. M. Welty, R. D. Long, J. R. Bailey, M. J. Parnell, N. P. Hoe, G. G. Adams, F. R. Deleo, and J. M. Musser.** 2005. Extracellular deoxyribonuclease made by group A *Streptococcus* assists pathogenesis by enhancing evasion of the innate immune response. Proc. Natl. Acad. Sci. USA **102:**1679–1684.
37. **Sumby, P., S. F. Porcella, A. G. Madrigal, K. D. Barbian, K. Virtaneva, S. M. Ricklefs, D. E. Sturdevant, M. R. Graham, J. Vuopio-Varkila, N. P. Hoe, and J. M. Musser.** 2005. Evolutionary origin and emergence of a highly successful clone of serotype M1 group A *Streptococcus* involved multiple horizontal gene transfer events. J. Infect. Dis. **192:**771–782.
38. **Sutcliffe, I. C., and D. J. Harrington.** 2002. Pattern searches for the identification of putative lipoprotein genes in Gram-positive bacterial genomes. Microbiology **148:**2065–2077.
39. **Szmelcman, S., M. Schwartz, T. J. Silhavy, and W. Boos.** 1976. Maltose transport in *Escherichia coli* K12. A comparison of transport kinetics in wild-type and lambda-resistant mutants as measured by fluorescence quenching. Eur. J. Biochem. **65:**13–19.
40. **Thomson, J., Y. Liu, J. M. Sturtevant, and F. A. Quiocho.** 1998. A thermodynamic study of the binding of linear and cyclic oligosaccharides to the maltodextrin-binding protein of *Escherichia coli*. Biophys. Chem. **70:**101–108.
41. **Virtaneva, K., S. F. Porcella, M. R. Graham, R. M. Ireland, C. A. Johnson, S. M. Ricklefs, I. Babar, L. D. Parkins, R. A. Romero, G. J. Corn, D. J. Gardner, J. R. Bailey, M. J. Parnell, and J. M. Musser.** 2005. Longitudinal analysis of the group A *Streptococcus* transcriptome in experimental pharyngitis in cynomolgus macaques. Proc. Natl. Acad. Sci. USA **102:**9014–9019.
42. **Vise, P. D., K. Kodali, N. Hoe, A. Paszczynski, J. M. Musser, and G. W. Daughdrill.** 2003. Stable isotope labeling of a group A *Streptococcus* virulence factor using a chemically defined growth medium. Protein Expr. Purif. **32:**232–238.
43. **Wandersman, C., M. Schwartz, and T. Ferenci.** 1979. *Escherichia coli* mutants impaired in maltodextrin transport. J. Bacteriol. **140:**1–13.